(4)

WOD/CO/HYDRO-87-09

EFFECTS ON ELECTROMAGNETIC WAVE PROPAGATION AND ROCKET VAPOR TRAILS OF INTENSE TURBULENCE GENERATED BY BREAKING INTERNAL GRAVITY WAVES

John R. Grant*
WESTINGHOUSE OCEANIC DIVISION
CLEVELAND OPERATION
Hydrodynamics Research and Technology
(formerly Ocean Systems Division
Gould Defense Systems, Inc.)
52 Johnnycake Hill
Middletown, Rhode Island 02840

14 August 1989

Final report for period August 1986 - September 1987
Contract N00014-86-C-0662

Prepared for
STRATEGIC DEFENSE INITIATIVE ORGANIZATION
Washington, D.C. 20301-7100

OFFICE OF NAVAL RESEARCH (CODE 1214)
Arlington, Virginia 22217

---

*Dr. Grant's present address is Naval Underwater Systems Center (Code 804), Newport, Rhode Island 02841

UNCLASSIFIED

SECURITY CLASSIFICATION OF THIS PAGE

REPORT DOCUMENTATION PAGE

1a REPORT SECURITY CLASSIFICATION UNCLASSIFIED	1b RESTRICTIVE MARKINGS NONE
2a SECURITY CLASSIFICATION AUTHORITY	3 DISTRIBUTION / AVAILABILITY OF REPORT APPROVED FOR PUBLIC RELEASE: DISTRIBUTION IS UNLIMITED.
2b DECLASSIFICATION / DOWNGRADING SCHEDULE	
4 PERFORMING ORGANIZATION REPORT NUMBER(S) WOD/CO/HYDRO-87/09 ✓	5 MONITORING ORGANIZATION REPORT NUMBER(S)
6a NAME OF PERFORMING ORGANIZATION WESTINGHOUSE OCEANIC DIVISION CLEVELAND OPERATION 6b OFFICE SYMBOL (If applicable)	7a NAME OF MONITORING ORGANIZATION OFFICE OF NAVAL RESEARCH (CODE 1214)
6c ADDRESS (City, State, and ZIP Code) HYDRODYNAMICS RESEARCH AND TECHNOLOGY 62 JOHNNYCAKE HILL MIDDLETOWN, RI 02840	7b ADDRESS (City, State, and ZIP Code) ARLINGTON, VA 22217
8a NAME OF FUNDING / SPONSORING ORGANIZATION STRATEGIC DEFENSE INITIATIVE ORGANIZATION 8b OFFICE SYMBOL (If applicable)	9 PROCUREMENT INSTRUMENT IDENTIFICATION NUMBER N00014-86-C-0662
8c ADDRESS (City, State, and ZIP Code) WASHINGTON, D.C. 20301-7100	10 SOURCE OF FUNDING NUMBERS PROGRAM ELEMENT NO: 63220 / PROJECT NO / TASK / WORK UNIT ACCESSION NO

11 TITLE (Include Security Classification)
(U) EFFECTS ON ELECTROMAGNETIC PROPAGATION AND ROCKET VAPOR TRAILS OF INTENSE TURBULENCE

12 PERSONAL AUTHOR(S)
JOHN R. GRANT

13a TYPE OF REPORT	13b TIME COVERED	14 DATE OF REPORT (Year, Month, Day)	15 PAGE COUNT
FINAL	FROM 08/86 TO 09/87	89 AUG 14	15

16 SUPPLEMENTARY NOTATION

17 COSATI CODES			18 SUBJECT TERMS (Continue on reverse if necessary and identify by block number)
FIELD	GROUP	SUB-GROUP	INTERNAL WAVES, TURBULENCE, LASER PROPAGATION

19 ABSTRACT (Continue on reverse if necessary and identify by block number)

This work aims to investigate the effects on laser propagation of turbulence produced by breaking internal gravity waves in the mesosphere. At the time of this writing the major parameter, C_n^2, needed for this investigation has been computed for a representative case. The case is a narrow-band wave generated at the ground and propagating upward; breaking eventually occurs over altitudes from less than 40 to greater than 93 kilometers, the upper limit of the calculation. The calculation itself, if not strictly from first principles, involves only a relatively small amount of approximation to the Navier-Stokes equations, both for the wave motion and the turbulence. The evolution of C_n^2 is followed from its inception in the breaking part of the wave phase, its growth in magnitude and coalescence across the phases, to its subsequent decay as the turbulence dies away. Peak values of about 10^{-17} $m^{-2/3}$ are observed in C_n^2. With these results, effects such as variance in intensity and phase, beam spread and beam wander may be computed.

20 DISTRIBUTION / AVAILABILITY OF ABSTRACT	21 ABSTRACT SECURITY CLASSIFICATION
☒ UNCLASSIFIED/UNLIMITED ☐ SAME AS RPT ☐ DTIC USERS	UNCLASSIFIED
22a NAME OF RESPONSIBLE INDIVIDUAL JOHN R. GRANT	22b TELEPHONE (Include Area Code) (401) 841-3546
	22c OFFICE SYMBOL NUSC 804

DD FORM 1473, 84 MAR 83 APR edition may be used until exhausted. All other editions are obsolete.

SECURITY CLASSIFICATION OF THIS PAGE
UNCLASSIFIED

TABLE OF CONTENTS

ABSTRACT

This work aims to investigate the effects on laser propagation of turbulence produced by breaking internal gravity waves in the mesosphere. At the time of this writing the major parameter, C_n^2, needed for this investigation has been computed for a representative case. The case is a narrow-band wave generated at the ground and propagating upward; breaking eventually occurs over altitudes from less than 40 to greater than 93 kilometers, the upper limit of the calculation. The calculation itself, if not strictly from first principles, involves only a relatively small amount of approximation to the Navier-Stokes equations, both for the wave motion and the turbulence. The evolution of C_n^2 is followed from its inception in the breaking part of the wave phase, its growth in magnitude and coalescence across the phases, to its subsequent decay as the turbulence dies away. Peak values of about 10^{-17} $m^{-2/3}$ are observed in C_n^2. With these results, effects such as variance in intensity and phase, beam spread and beam wander may be computed.

LIST OF FIGURES

1. INTRODUCTION

The turbulence generated by breaking internal gravity waves may be sufficient to require consideration in operation strategies and equipment design for high energy laser propagation. This report summarizes the work on such turbulence and its effects on laser beam propagation during the period 1986 - 1987, while the author was employed at Gould Ocean Systems Division.

A central focus of the research has been the numerical calculation of breaking internal waves and the associated turbulence using a code previously written especially for this purpose. The results presented below are from two sets of calculations. In one set the gravity waves are made to break by their propagation upward into less and less dense air; the breaking occurs over a height layer ranging from less than 40 to greater than 90 km. Peak values of C_n^2 of about 10^{-17} $m^{-2/3}$ are found. In the second set breaking is induced by an encounter of a wave with its critical level. This more idealized calculation is relevant to all levels of the atmosphere. For the density of the atmosphere at the tropopause (e.g., in the case when a wave has a critical level on the upper side of the jet stream -- a not uncommon event), the latter calculation yields peak values of C_n^2 of about 10^{-14} $m^{-2/3}$. These values of C_n^2 are consistent with those values observed with Doppler radar.

2. COMPUTATIONAL RESULTS

In the first set of calculations, the Brunt-Vaisala frequency and wind are uniform with height, having the values 0.0173 sec^{-1} and 13 m/sec, respectively. This uniformity in the background profiles allows the physics of the wave-breaking to be addressed without complicating factors due to the variation of these profiles. The density scale height is, thus, H = 9.33 kilometers, and this value is used to scale the height displayed in the plots presented next. The wave is forced at the lower boundary (i.e., the ground) by a motionless sinusoidal corrugation so that the wave has a wavelength of 50 kilometers, an amplitude of its horizontal component of induced velocity of 1.75 m/sec, and a phase speed c = 0.

The calculations discussed here maintain only this fundamental wavelength and so are 'quasilinear'. Subsequent calculations will include the shorter length modes generated in the wave (as opposed to turbulent) flow during breaking.

From the values given here, the time for the wind to travel one wavelength of the corrugation, or the wave 'period', is 50000/13 = 3846 sec = 64.1 minutes. The calculations shown were carried out to 17 periods. Figure 1 shows the wave-induced horizontal velocity u versus height at a single phase of the wave at 17 periods. The velocity is nondimensionalized by the original uniform wind speed. The wave has propagated to an altitude greater than 12.5 scale heights, and its magnitude increases markedly as it propagates into less and less dense air. This calculation was done with the turbulence turned off.

Breaking occurs when the wave amplitude is large enough that it pulls warm air beneath cool, and vice versa, setting up an unstable configuration. A convenient measure of whether the wave amplitude is large enough to cause breaking is the ratio of the magnitude of the horizontal component of wave-induced velocity to the intrinsic wave phase speed (the phase speed relative to the wind). Breaking occurs when this ratio exceeds unity. At the ground this ratio is, from the values given above, 1.75/13.0 = 0.135, so the wave is far from breaking when it is generated. However, as seen in Figure 1, the wave amplitude is much larger at altitude. The intrinsic phase speed also varies with height, being smaller at lower altitudes and larger at higher, than it is at the ground. Thus this ratio varies more slowly than the wave amplitude itself. In fact, as seen in Figure 2 where it is plotted, the ratio is nearly constant with height over a large height range. In this figure, the height range where this ratio exceeds unity is where breaking should occur. It is seen in the figure that the ratio exceeds one over several scale heights in a relatively short time interval (less than a period). This result predicts that breaking would begin to occur over this height range in a similarly short interval.

An exactly similar calculation was carried out, except that the turbulence computations were included. Turbulence generation by the wave breaking does indeed occur, with turbulence produced by about 15.5 periods into the calculation, as predicted by the behavior of the ratio shown in Figure 2. Figure 3 shows the wave-induced horizontal velocity versus height a one wave phase at 17 periods for this turbulent case. Note by comparing to the similar plot in Figure 1 how the turbulence in the height range of about 4 to 8 scale heights has reduced the wave amplitude, relative to the non-turbulent case.

As noted above, a main point of interest is the effect of this production of turbulence on electromagnetic wave propagation. To begin an investigation of this effect using these calculational results, the refractive index structure function C_n^2 has been computed for this case. Contours of C_n^2 versus height and horizontal distance over one wavelength at a time of 16.25 periods are given in Figure 4. Note how the turbulence -- as revealed by the structure function -- is already well-developed over a layer several scale heights deep. The wave phase propagation and advection of the turbulence by the wind and the wave itself result in a rather complex turbulence field. More details of C_n^2 may be seen in Figure 5, where a plot of C_n^2 versus height at a single wave phase (the phase at the left-hand boundary in Figure 4) is shown. This plot shows the vigorous, recently produced turbulence at a altitude of about 8 scale heights and slightly older, already decaying turbulence in the 5 ~ 6 scale height range. The narrow peaks which characterize this profile would be detected by radar as a succession of thin layers lying one above the other.

A second set of calculations has been used to study wave breaking caused by encounter with a critical level (the height where the component of the wind velocity in the direction of wave phase propagation equals the wave phase speed). Since the intrinsic phase speed is by definition zero at a critical level, the ratio of horizontal wave velocity amplitude to intrinsic phase speed (discussed above and shown in Figure 2 for that case) should become infinite according to linear theory. Hence critical levels are widely recognized to be sites of strong turbulence production.

Figures 6 and 7 display results from this set of calculations. In these calculations the wave is generated at the lower boundary ($z = -4$) with a phase speed $c = 0$. The wind is specified by the hyperbolic tangent function, so the critical level is at $z = 0$. The wavelength is 12.56 kilometers. The wave begins to break at about 2.5 periods. Figure 6 shows contours of C_n^2 one period later at 3.5 periods. The breaking has taken place just below the critical level, and the concentrated peaks in C_n^2 at about $z = -1$ reflect the sharp density gradients caused by the downward plunge of the wave into the air below its crest.

3. CONCLUDING REMARKS

A goal of this research is to include features of the atmosphere that materially effect the behavior of the wave breaking and hence the turbulence production and its effects on laser propagation. One such feature is the broad-banded spectral nature of many atmospheric waves, as opposed to the single wavelength calculations presented above. Figure 7 shows some results from a simulation where the forced wave had a broad-band spectrum. Plotted there are contours of potential temperature for a calculation where the wave forcing at the lower boundary was over a band of wavelengths rather than the single wavelength forced in the above calculations. At the time of the plot the wave was just on the verge of breaking, as can be seen by the vertical temperature contour at about $x = 0.5$, $z = -1$. From this plot it appears that the more complicated wave spectrum will lead to smaller pockets of breaking, rather than a single layer where breaking takes place. Future work will investigate this behavior more fully.

All of these results will be used to assess the effects of such turbulence on high energy laser propagation. For example, r_o, the first moment of C_n^2 (i.e., the integral of zC_n^2 over heights) is an important quantity for this assesment, and can be readily computed from the results shown. A key quantity is the ratio of the laser beam intensity with out turbulence to that with turbulence, and this will be computed versus time for the wave breaking cases calculated.

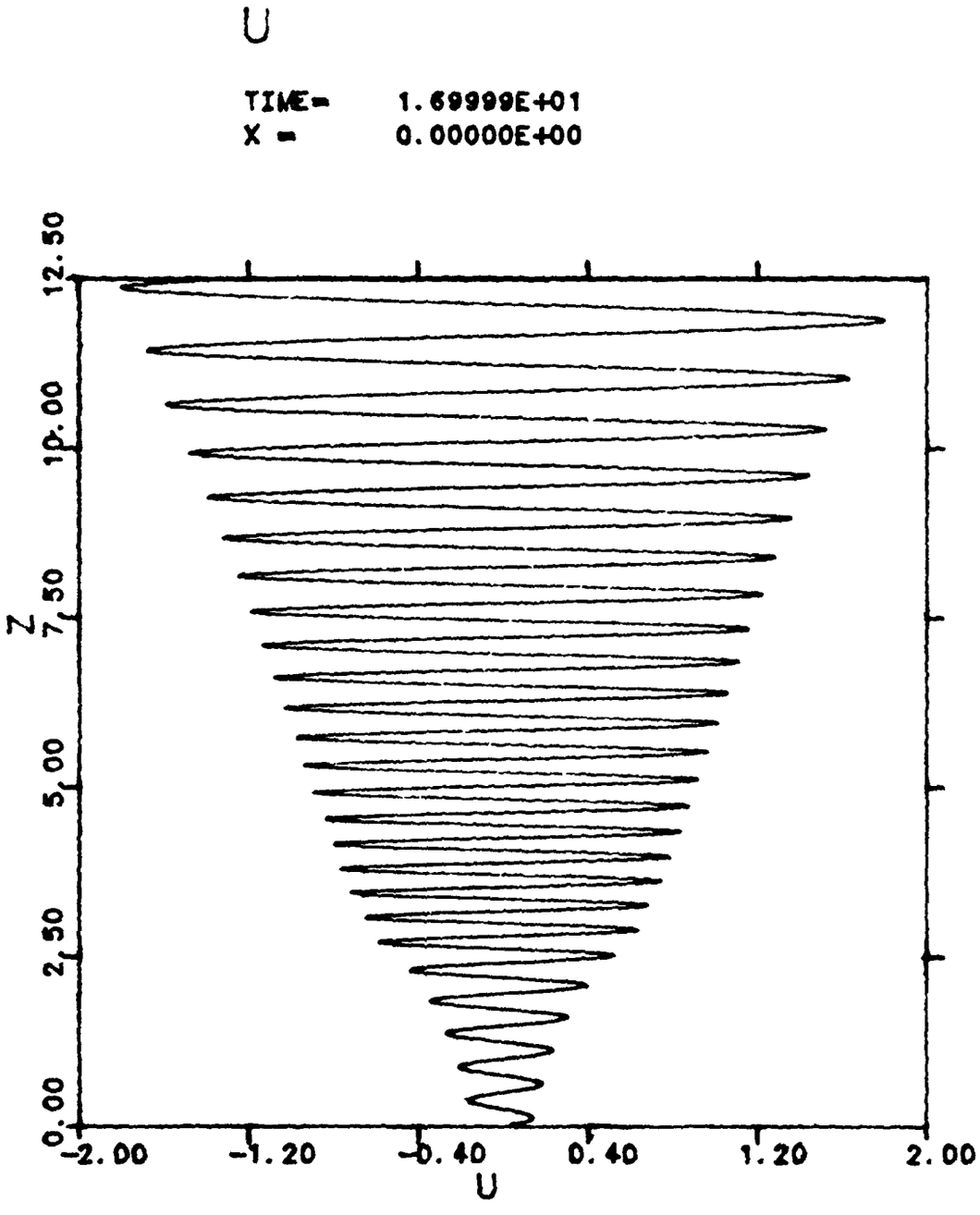

Figure 1. Non-turbulent calculation: Plot of horizontal component of wave-induced velocity versus height. At t = 17 periods, horizontal phase = 0. Height nondimensionalized by the density scale height = 9.33 km and velocity nondimensional by the initial uniform wind speed = 13 m/sec.

JRG/sg/2905m/9-87

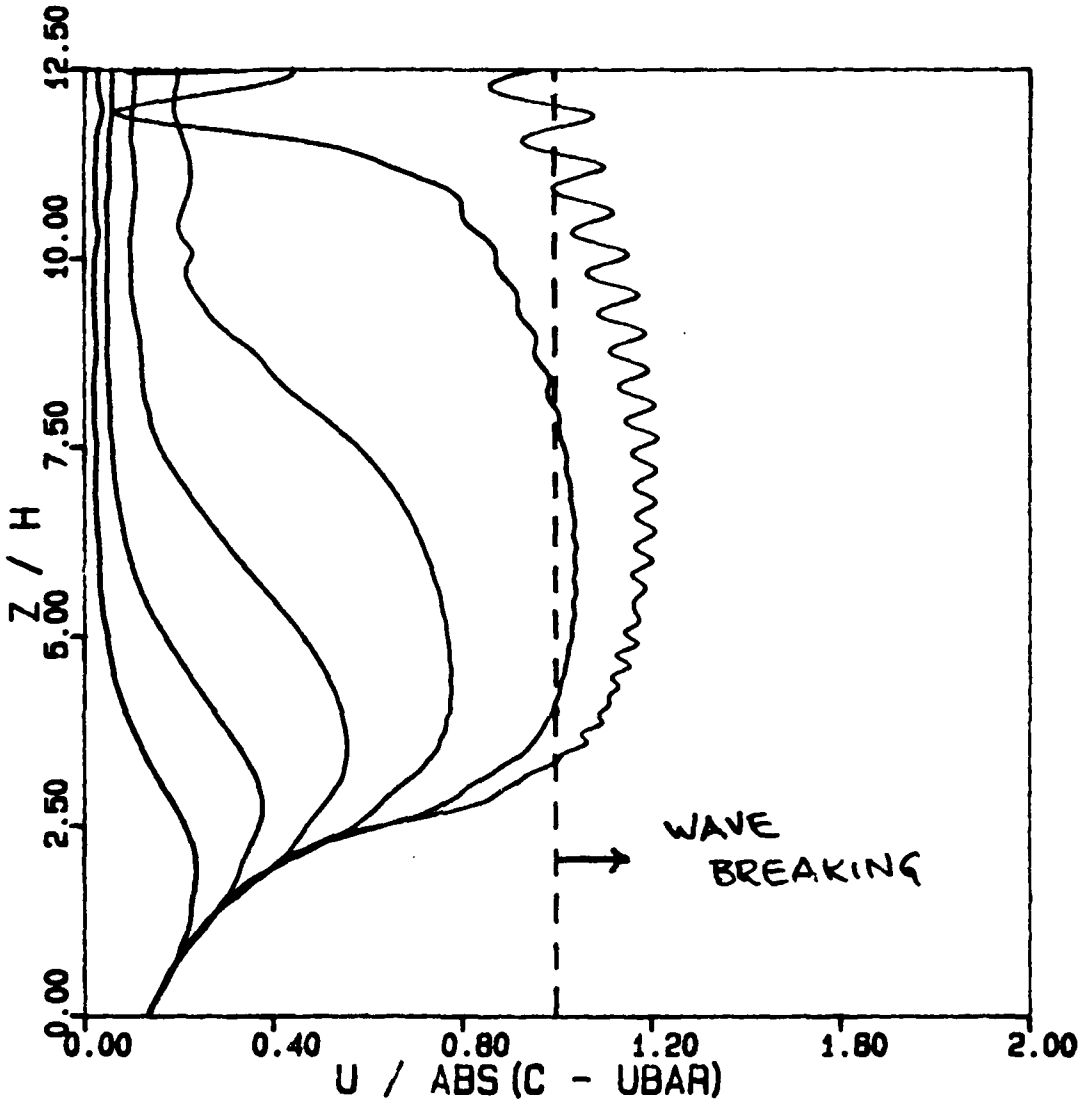

Figure 2. Non-turbulent calculation: Plot versus height of the ratio of the amplitude of the horizontal component of wave-induced velocity divided by the intrinsic phase speed at 8(a), 10(b), 12(c), 14(d), 16(e), 17(f) periods. Height nondimensionalized by the density scale height = 9.33 km.

JRG/sg/2905m/9-87

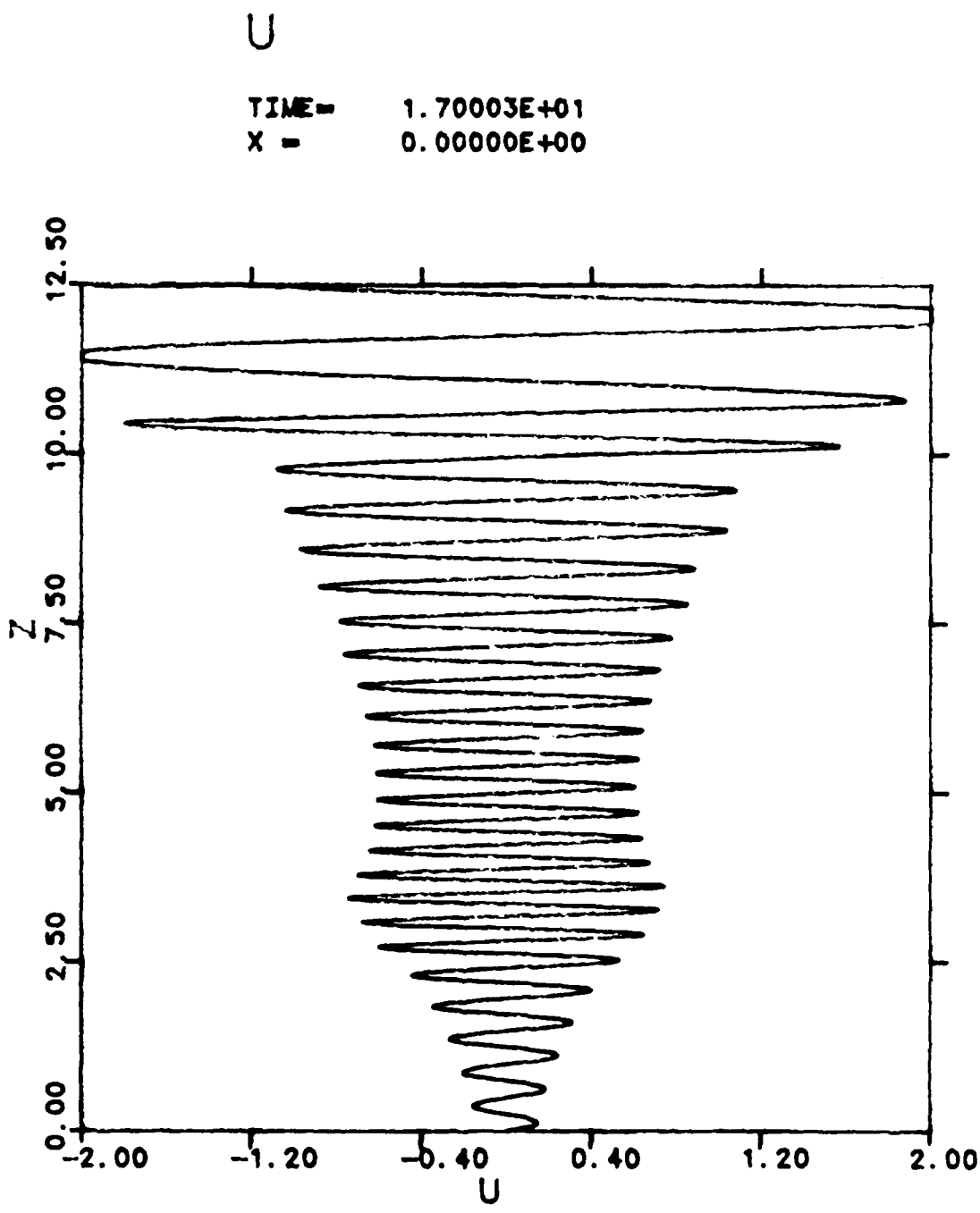

Figure 3. Turbulent calculation: Plot of horizontal component of wave-induced velocity versus height. At t = 17 periods, horizontal phase = 0. Height nondimensionalized by the density scale height = 9.33 km and velocity nondimensional by the initial uniform wind speed = 13 m/sec.

JRG/sg/2905m/9-87

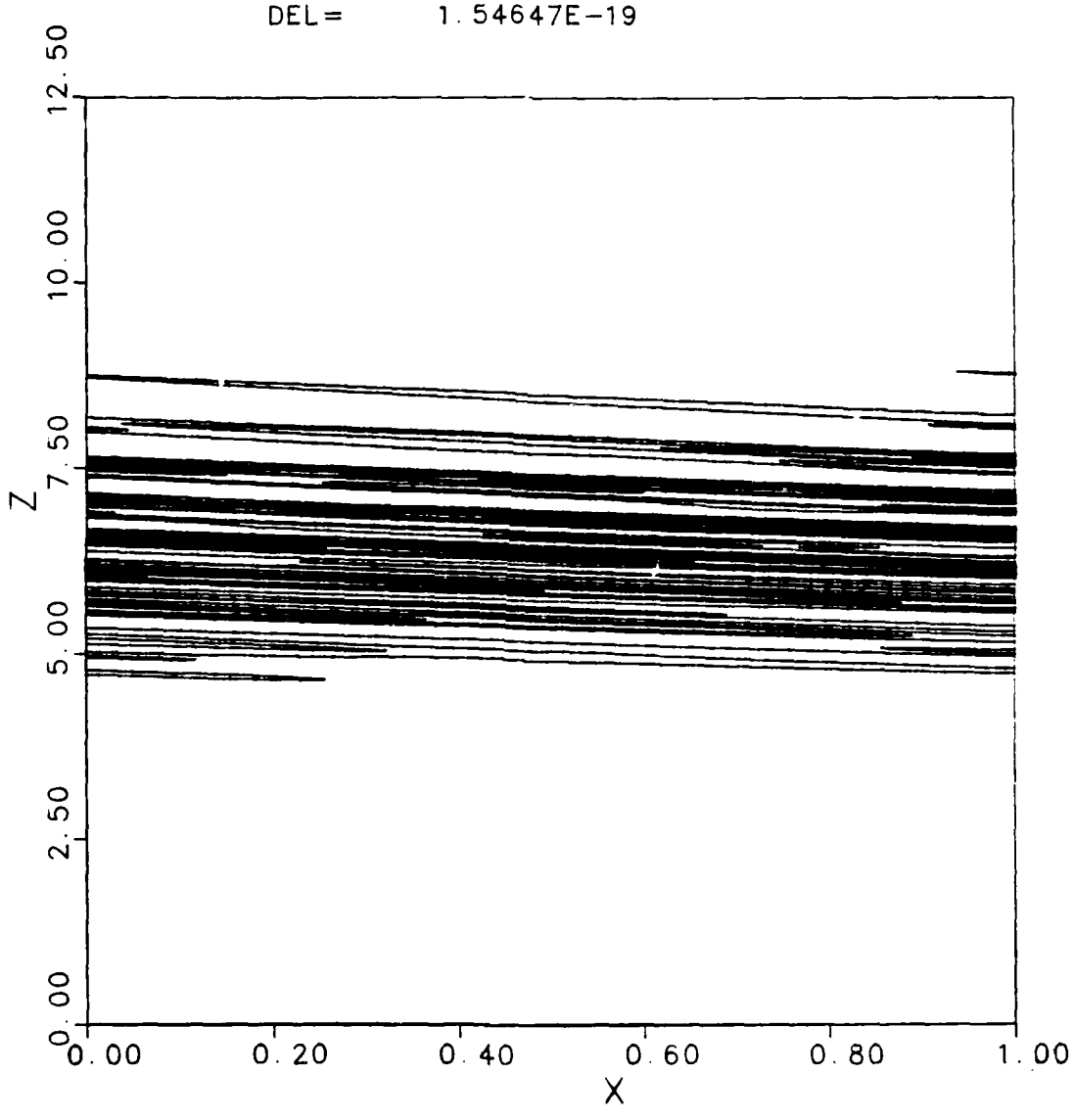

Figure 4. Turbulent calculation: Contour plot of C_n^2 at t = 16.25 periods. The x-axis covers 1 wavelength = 50 km. Units of C_n^2 are $m^{-2/3}$.

JRG/sg/2905m/9-87

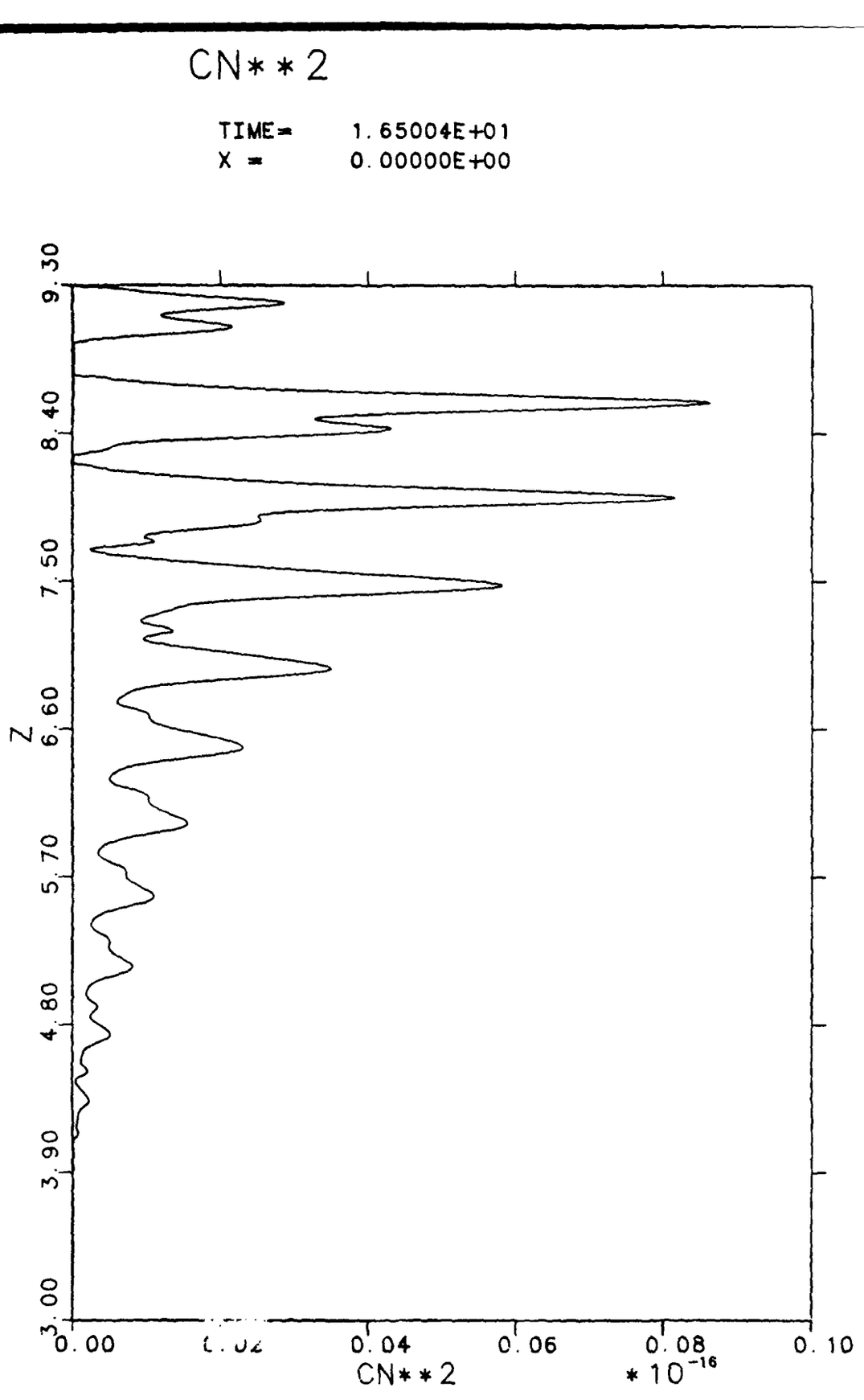

Figure 5. Turbulent calculation: Plot of C_n^2 (in $m^{-2/3}$) versus height. Height is nondimensionalized by the density scale height = 9.33 km.

JRG/sg/2905m/9-87

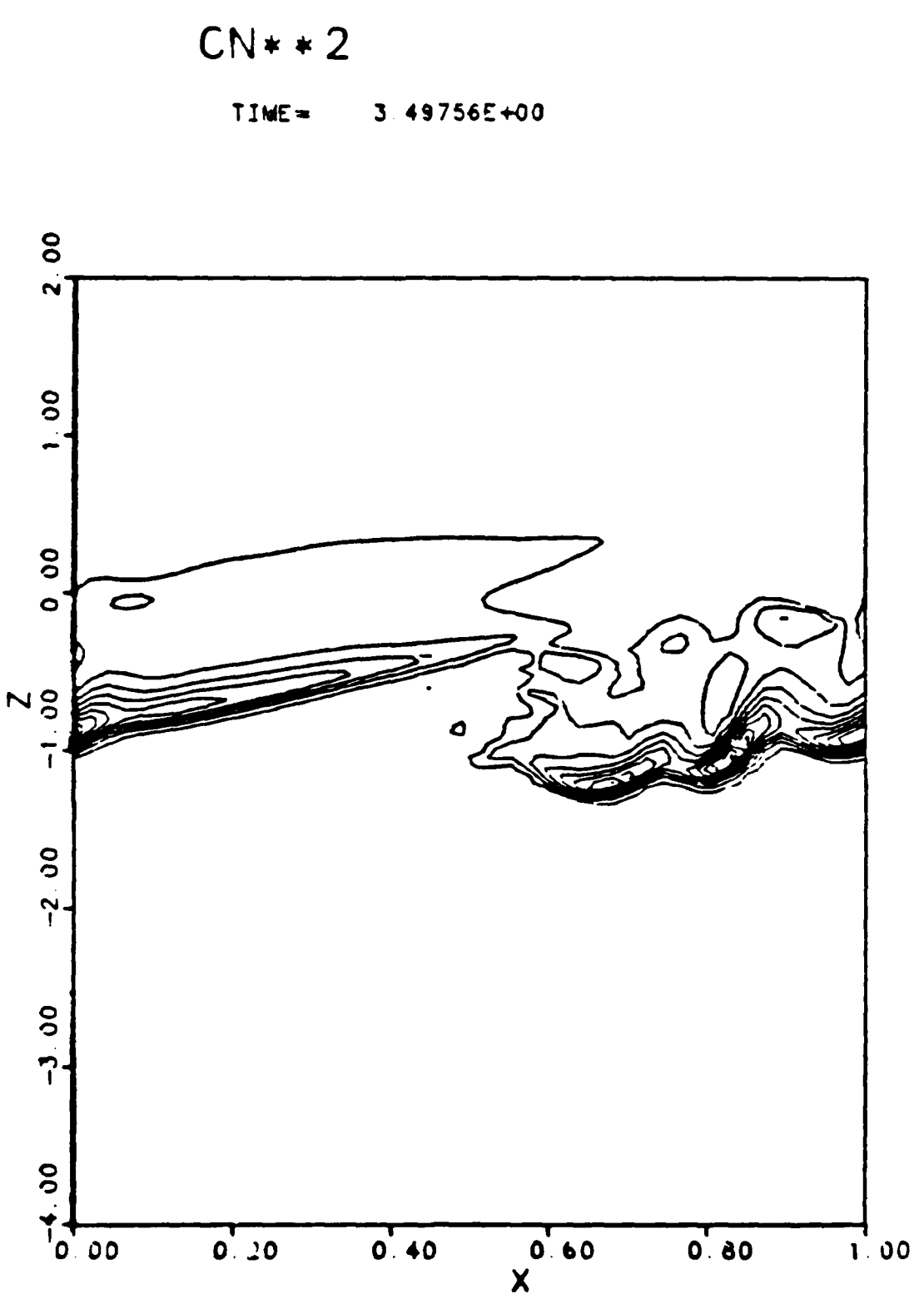

Figure 6. Contour plot of C_n^2 at t = 3.5 periods for the critical level encounter calculation. Height nondimensionalized by shear layer half-thickness = 1 km. The x-axis covers 1 wavelength = 12.56 km.

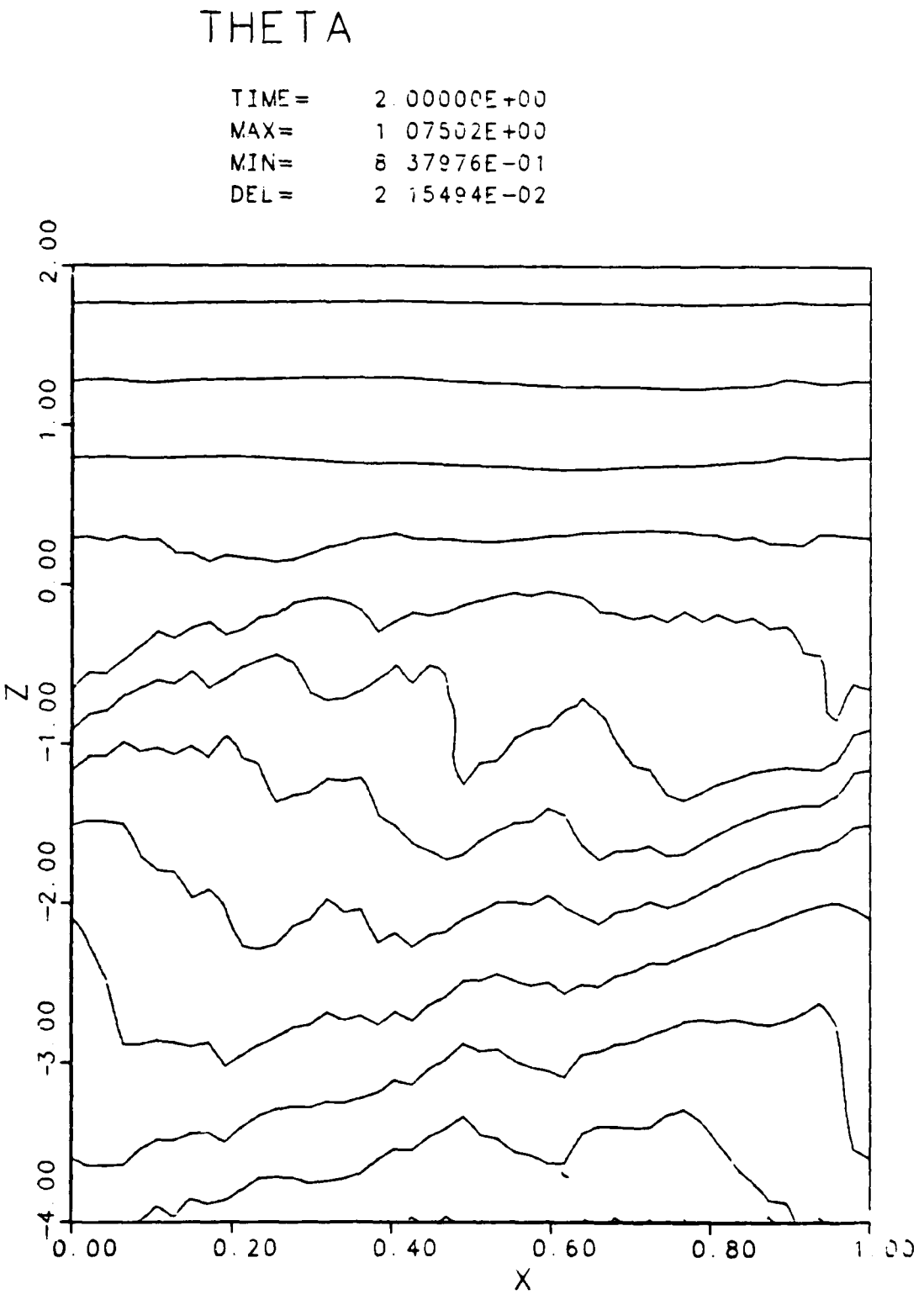

Figure 7. Contour plot of total (mean plus wave) potential temperature for the critical level encounter for a broad-band wave spectrum. Height nondimensionalized by shear layer half-thickness = 1 km. The x-axis covers 1 wavelength = 12.56 km.

JRG/sg/2905m/9-87